Analysis of Wave Packet Motion in Frequency and Time Domain: Oxazine 1

Markus Braun,* Constanze Sobotta, Regina Dürr, Horst Pulvermacher, and Stephan Malkmus

Lehrstuhl für BioMolekulare Optik, Department für Physik, Ludwig-Maximilians-Universität München, Oettingenstrasse 67, D-80538 München, Germany

Received: December 28, 2005; In Final Form: June 16, 2006

Wave packet motion in the laser dye oxazine 1 in methanol is investigated by spectrally resolved transient absorption spectroscopy. The spectral range of 600−690 nm was accessible by amplified broadband probe pulses covering the overlap region of ground-state bleach and stimulated emission signal. The influence of vibrational wave packets on the optical signal is analyzed in the frequency domain and the time domain. For the analysis in the frequency domain an algorithm is presented that accounts for interference effects of neighbored vibrational modes. By this method amplitude, phase and decay time of vibrational modes are retrieved as a function of probe wavelength and distortions due to neighbored modes are reduced. The analysis of the data in the time domain yields complementary information on the intensity, central wavelength, and spectral width of the optical bleach spectrum due to wave packet motion.

1. Introduction

Spectroscopy of vibrational wave packet dynamics is a modern tool to monitor coherent nuclear motion in molecular systems. The vibrational coherence induced by a short optical pulse is observed immediately after excitation and can therefore elucidate the energetic and structural changes in the very beginning of a photochemical reaction.[1−3] Moreover, in the coherent quantum control scheme[4] tailored wave packets are explored recently in order to influence the path of these photoreactions. Therefore exact knowledge about vibrational wave packets is mandatory for those experiments. The optical addressability of distinct vibrational modes together with the decay time of the vibrational coherence limits the spectral and temporal window in which coherent control experiments can take place.

Because of different equilibrium conformations in the ground and the excited states, the broadband optical excitation of a molecule in the Franck−Condon region with an ultra-short pulse generates a vibrational wave packet on a steep part of the excited-state potential-energy surface. By a Raman-like interaction, the excitation pulse can also lead to coherence in the electronic ground state forming a ground-state wave packet.[5,6] In a simple picture, the molecular wave packet evolves on a single vibrational coordinate and the molecule undergoes no reaction to product states. In this case the wave packet moves back and forth in the ground/excited-state parabola. Therefore the optical properties of the molecule connected to the electronic state in which the wave packet evolves are modulated with that vibrational frequency. Sensitive optical transitions for the study of vibrational wave packets are for example the induced absorption, stimulated emission, and bleaching of the ground-state absorption.

The most powerful tool of the experimentalist to observe vibrational wave packet motion in real time is femtosecond time-resolved pump−probe spectroscopy. Here the cross-correlation width of pump and probe pulse determines the temporal resolution and therefore the upper limit of the vibrational frequency range accessible for the experiment. The progress in pulse generation, amplification, and compression in the last years made tunable pulses in the 10-fs range available from the near UV to the IR spectral range.[7−9] Therefore the investigation of vibrational wave packets in the interesting frequency ranges up to 2000 cm^{-1}, where most of the indicative molecular modes are found, is feasible.

In a transient absorption experiment, the effect of wave packet dynamics is observed as an oscillatory component overlaying the kinetics determined by changes in population. In a standard evaluation, the usually slower population kinetics and possibly a dynamic Stokes shift due to the solvent are subtracted from the original data set. The remaining residuum of the transient absorption signal contains only the oscillatory part of the transient absorption signal. In the standard procedure of data evaluation, a Fourier transformation (FT) of that residuum yields the spectrum of the vibrational modes associated with the wave packet. With this common treatment, frequency, amplitude, phase, and decay times of the vibrational modes are extracted from the measured data set. Problems may arise when a weak vibrational mode in the vicinity of a stronger one has to be analyzed. Amplitude, spectral position, and width of the weak mode will be distorted due to interference effects as outlined below.

In addition, an unambiguous assignment of the vibrational FT spectrum to either the ground state or excited state is not always straightforward. Especially for systems where the probed molecule experiences a small dynamic Stokes shift, the absorption and emission spectra overlap in a broad spectral range. Therefore a simple assignment of the modes according to the probe wavelength is not possible.

Interesting information is expected from the analysis of the phase of the oscillations. When the wave packet oscillates on the potential-energy surface, the central wavelength of the respective optical transition oscillates correspondingly. This leads to a phase shift of π between the oscillations monitored on the red and blue edges of the signal and a reduction of the oscillation intensity at the mean wavelength. In practice the

* To whom correspondence should be addressed. E-mail: markus.braun@physik.uni-muenchen.de. Fax: ++49 +89 2180 9202.

10.1021/jp057543l CCC: $33.50
Published on Web 07/20/2006

SCHEME 1

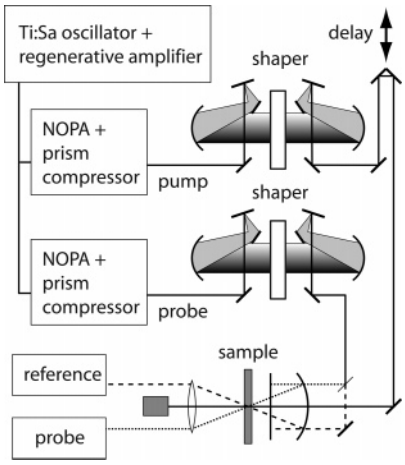

phase determination proves to be very demanding from an experimental point of view. A reliable determination of the phase requires knowledge of the time-zero function with high accuracy. Phase analysis of the wave packets especially in the spectral overlap region between absorption and emission with only slightly frequency shifted vibrational modes in the ground and excited state does not lead to unambiguous results.[10,11]

In this study, we present transient absorption data on the laser dye oxazine 1 in methanol. The influence of the wave packet motion on the optical transitions is investigated by using data evaluation methods in the time and frequency domain. We introduce a FT evaluation algorithm that allows the determination of frequency, amplitude, and decay time of vibrational wave packet modes even in the vicinity of a stronger one. For a further evaluation method in the time domain, a Gaussian fit of the transient absorption spectra as a function of delay time is applied to the data. The contributions of optical frequency shift and optical transition dipole moment to the observed oscillatory component in the transient absorption measurement are separated by evaluating the width, amplitude, and spectral position of the Gaussians.

2. Materials and Methods

The laser system for the transient absorption measurements[12] consists of a home-built Ti:Sapphire oscillator (100-MHz repetition rate, 20-fs pulse duration, 10-nJ pulse energy) and a regenerative amplifier (1-kHz repetition rate, 80-fs pulse duration, 350-μJ pulse energy) at a central wavelength of 800 nm (see Scheme 1). The output of the laser is used to pump two NOPAs (noncollinear optical parametric amplifier)[7−9] that deliver pump and probe pulses for the transient absorption measurements. During the fine tuning of the NOPA process, particular attention was paid to obtain preferably unstructured spectral profiles of the pulses in order to reduce pre- and afterpulses (see Figure 1c). The pulses were compressed by a combination of a quartz prism compressor and pulse shaper (with 256-pixel liquid−crystal phase and amplitude modulator in a 4f-geometry zero-dispersion) to pulse durations of 13 and 15 fs, respectively. The pulses were characterized by measuring the spectrum, autocorrelation, and cross-correlation frequency-resolved optical gating (FROG). The group velocity dispersion (GVD) of pump and probe pulse is shown in Figure 1c.

For the measurement of the transient absorption signal the output of one NOPA was split in two parts, the probe pulse and a reference pulse. Both pulses pass the sample at the same position, but the reference pulse travels through the sample about

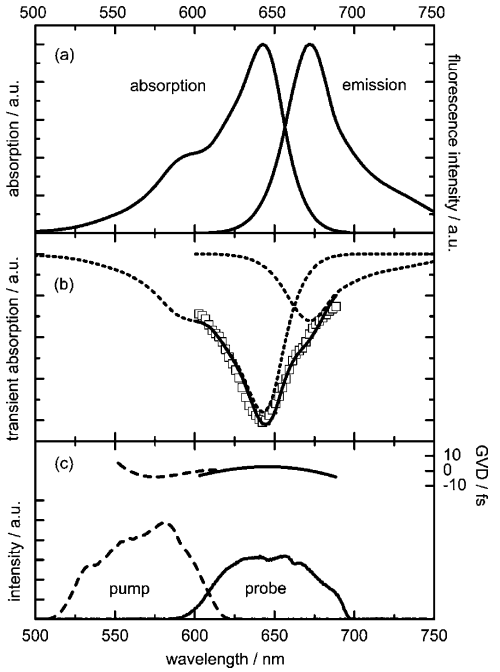

Figure 1. (a) Steady-state absorption $A(\lambda)$ and fluorescence $F(\lambda)$ spectrum of oxazine 1 dissolved in methanol (normalized spectra plotted as $A(\lambda)\cdot\lambda$ and $F(\lambda)\cdot\lambda^3$). (b) Nanosecond component of the transient absorption signal as obtained from global fit (squares) and a linear superposition (thick line) of absorption and emission spectrum (dotted lines). The spectrum of the long-lived transient absorption signal is reproduced by the steady-state absorption spectra. (c) Spectrum of pump pulse (duration of 13 fs at 570 nm) and probe pulse (duration of 15 fs at 650 nm). Above, the GVD of pump (dotted line) and probe (solid line) pulses is shown as determined by cross-correlation FROG measurement.

1 ns in advance of the probe pulse. The transmitted light of both pulses is spectrally resolved by two identical spectrometers. The spectra are recorded with two photodiode arrays (42 elements each) that are read out with 1-kHz repetition rate in order to realize single-pulse detection. The sample is photoexcited by the output of the second NOPA that delivers the pump pulse. The delay between pump and probe pulse is varied by a mechanical delay stage.

The laser dye oxazine 1 was purchased by Lambda-Physik and dissolved in methanol (Merck, p.a.) without further purification. Ten milliliters of this solution was pumped through a quartz flow cell (thickness 50 μm) to exchange the excitation volume completely after each laser shot. The small thickness of the flow cell ensures that no group velocity effects influence the pulse parameter during the excitation and probing process. The concentration of oxazine 1 was chosen to yield an optical transmission of 10% at the absorption maximum at 643 nm in the 50-μm cuvette.

Resonance Raman data (Figure 4) of oxazine 1 was recorded by steady-state excitation with a HeNe laser. For these measurements, oxazine 1 was dissolved in DMA to quench the spontaneous fluorescence.[13]

3. Results

In Figure 1 the spectral properties and slow kinetics of oxazine 1 in methanol are summarized. Figure 1a shows the normalized steady-state absorption $A(\lambda)$ and fluorescence $F(\lambda)$ spectra of the sample (plotted as $A(\lambda)\cdot\lambda$ and $F(\lambda)\cdot\lambda^3$) which peak at 643 and 672 nm. In Figure 1b the long-lived nanosecond component of the transient absorption spectrum (described below) is shown. This spectral signature can be nicely repro-

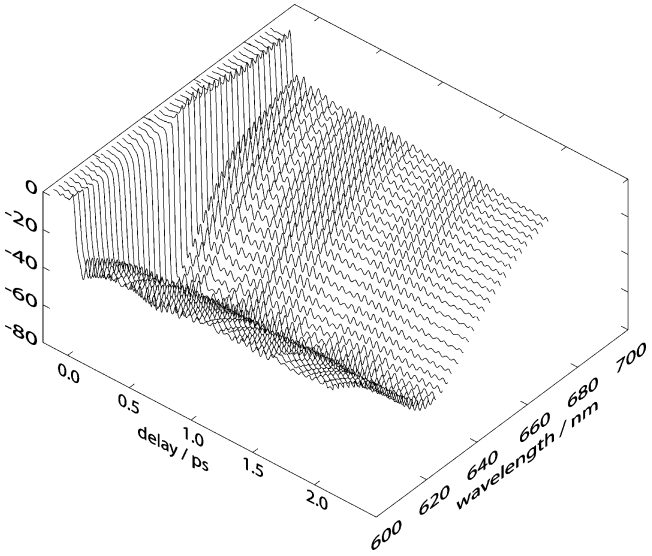

Figure 2. 3-D plot of transient absorption signal as a function of probe wavelength (600−690 nm) and delay time (−0.1 to 2.1 ps). At a delay time of 0.0 ps an immediate negative transient absorption signal of up to −80 mOD is observed, that peaks at about 647 nm. The transient absorption signal is modulated with an amplitude of about 10 mOD and a main period of about 60 fs.

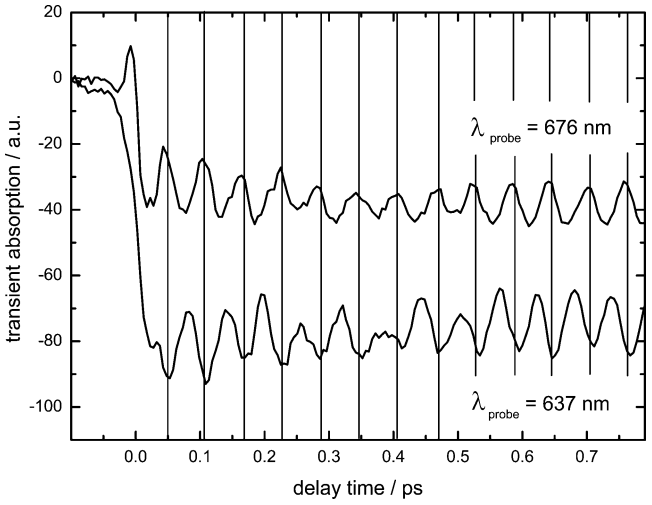

Figure 3. Transient traces recorded for probe wavelengths of 676 and 637 nm. The oscillation on the transient absorption shows an obvious phase jump of π.

duced by a linear superposition of the steady-state absorption and fluorescence spectra, which identifies the spectral range where absorption bleach (λ < 680 nm) and stimulated emission (λ > 630 nm) signals are observed. The spectra of pump and probe pulse used for the transient absorption studies are presented in Figure 1c. The probe pulse (600−690 nm) covers the spectral region where ground-state bleach and stimulated emission signals are partially overlapping.

In Figure 2, the transient absorption spectrum of oxazine 1 in methanol in that wavelength range recorded over 2 ps is shown. Immediately after excitation of the sample, a long-lived transient absorption signal over the whole spectral range is observed (see also Figure 1b). On this signal a fast oscillatory component with a period of about 60 fs is noticed that shows a beating behavior with a period of about 650 fs. This indicates at first glance the presence of two dominant vibrational modes at around 600 cm^{-1}, which are separated by about 50 cm^{-1}. By comparison of transient traces on the blue and red wings of the transient absorption spectrum at 637 and 676 nm (see

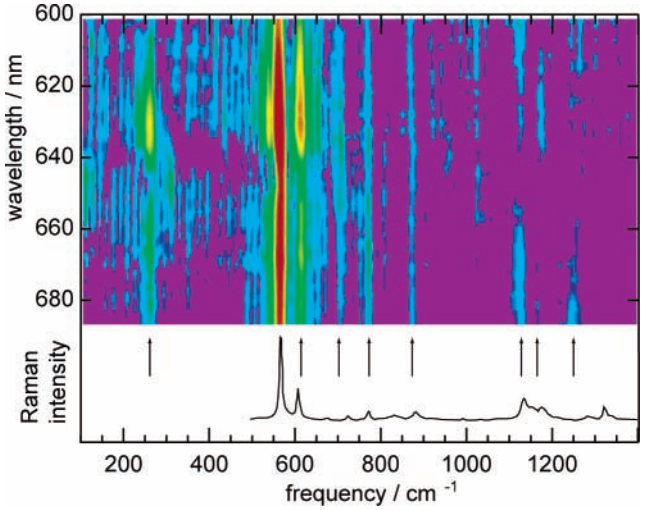

Figure 4. Fourier transformed data set of the transient absorption data, as described in the text. The Fourier amplitude (in a color code) is plotted against the probe wavelength and vibrational frequency. For comparison also the Raman spectrum is plotted, below. The vibrational modes as obtained from the evaluation algorithm for a probe wavelength of 637 nm are: 260.2, 560.8, 606.6, 695.1, 768.1, 872.4, 1126.2, 1172.7, and 1249.5 cm^{-1}, also denoted by arrows. Also observed is a vibrational mode at 1030 cm^{-1}, which is assigned to the solvent (C−O stretch of methanol).

Figure 3), a phase shift of π for the oscillations can be seen. The amplitude of the oscillations decreases with a time constant of about 2 ps. Beside these immediate observations on the data in the time domain a more thorough analysis is achieved by the investigation of the FT data set in the frequency domain.

For a quantitative evaluation of the data the following procedure was applied for all data sets. The long term behavior of the transient absorption signal (Figure 1b) was determined in a global fitting routine by an exponential fit of the data using the measured cross correlation function of pump and probe pulse from the FROG experiment. After subtracting the slow population kinetics with a time constant of several nanoseconds from the original data a residuum remains that yields only the fast oscillatory part of the signal on a zero signal offset. To exclude effects of any time-zero artifacts, only the data for delay times longer than 50 fs was used in the following procedure. For an analysis in the frequency domain the time-resolved residuum data set was Fourier transformed. This procedure yields the wavelength-dependent frequency spectrum of the observed oscillations as shown in Figure 4, where the intensities are displayed in a color code.

As can be seen in Figure 4, the two dominant vibrational modes, which are also responsible for the beating behavior in the transient traces, are about 560 and 609 cm^{-1}. The general frequency of the time-resolved traces leads to a period of $T = (c \cdot 560\ cm^{-1})^{-1} = 59.5$ fs (see Figure 3). The beating behavior is explained by the frequency difference of the 560 and 609 cm^{-1} modes of $\Delta\nu = 49\ cm^{-1}$ leading to a period of $T_{beat} = (c \cdot 49\ cm^{-1})^{-1} = 680$ fs, which was noticed in the transient traces (Figures 2 and 3). Also several other weaker modes (indicated by arrows in Figure 4) are visible in the FT data set. For comparison the resonance Raman spectrum of oxazine 1 in DMA is also shown and good agreement between the modes from the transient absorption measurement and the Raman method is found.

Nevertheless, a closer look at the FT data set reveals a number also strong periodic side maxima and asymmetric line shapes. These additional features will be analyzed and used to gain

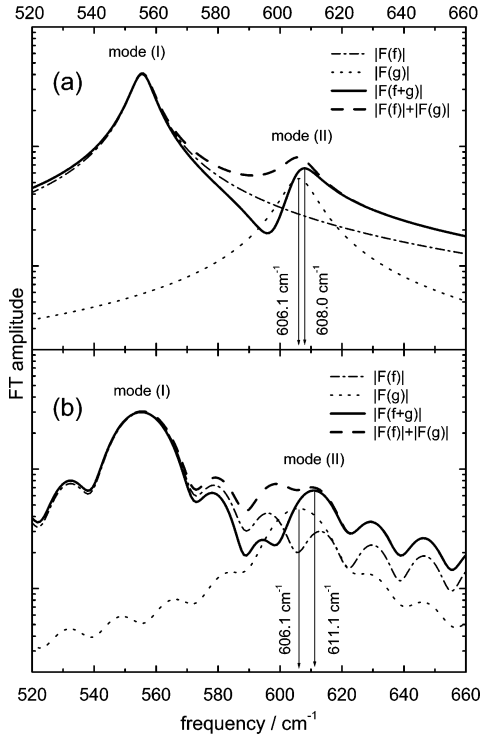

Figure 5. Demonstration of interference effects between neighbored vibrational modes in a FT spectrum (the FT amplitude is plotted on a logarithmic scale): FT amplitude of mode i at 555.6 cm^{-1} and a decay time of 1.5 ps (dash−dotted line); FT amplitude of mode ii at 606.1 cm^{-1} and a decay time of 1.0 ps (dotted line); FT amplitude of the sum of modes i and ii (thick line), denoted as iii; sum of the FT amplitudes i and ii (thick dashed line), denoted as iv. (a) The data sets in the time domain extend over about 41 ps. (b) the data sets in the time domain extend over 2.1 ps. Therefore the Lorentzian profiles in b are convoluted with a sinc function due to the finite temporal range. The line profile of the FT data set iii is in both cases strongly distorted, asymmetric, and shifted, as indicated by the arrows.

further information on the wave packet motion (see section A). Because of the side maxima of a strong mode, the mode parameters of weak neighbored modes can be influenced significantly. We will show that the simple procedure of just fitting the FT vibrational spectrum by a sum of Lorentzians with different spectral position, amplitude, and width can lead to distorted results.

A. Evaluation Algorithm for the Data in the Frequency Domain. The effect of interference between two neighbored vibrational modes in the FT amplitude spectrum will be illustrated on simulated data sets (Figure 5). The mode parameters were chosen to be similar to the oxazine 1 data set presented above. We generated two data sets in the time domain that describe the vibrational modes I and II

$$f(t) = 1.0 \exp(-t/1500\ \text{fs}) \sin(2\pi t/60\ \text{fs});\ t \geq 0$$

$$g(t) = 0.2 \exp(-t/1000\ \text{fs}) \sin(2\pi t/55\ \text{fs});\ t \geq 0 \quad (1)$$

Data set I describes one strong oscillatory mode with a period of 60 fs (555.6 cm^{-1}) and a decay time of 1500 fs. Data set II describes a weaker oscillation with a period of 55 fs (606.1 cm^{-1}) and a decay time of 1000 fs. In a typical transient absorption measurement, the sum of these two modes would be observed in time domain. Like in a real measurement, these two data sets were generated as a list of discrete delay times with a step size of 5 fs between two data points. Each data set consists of 8192 values, so it starts at a delay time of 0 fs and ends at a delay time of 40955 fs.

Figure 5a depicts in the frequency range between 520 and 660 cm^{-1} the FT amplitudes of four data sets on a logarithmic scale: the FT amplitude $|F(f)|$ of data set I, the FT amplitude $|F(g)|$ of data set II, the FT amplitude $|F(f + g)|$ of their sum, and the sum of their FT amplitudes $|F(f)| + |F(g)|$.

The two modes at 555.6 and 606.1 cm^{-1}, $|F(f)|$ and $|F(g)|$, are both found to have symmetrical Lorentzian shapes due to their decay times of 1500 and 1000 fs. By comparing them to the FT amplitude of their sum $|F(f + g)|$, one finds the mode parameters to be changed evidently, especially for the weak mode II. The center frequency is shifted by 1.9 cm^{-1} to 608.0 cm^{-1}; the line shape is strongly asymmetric and the amplitude of the mode is increased. For the strong mode (I), no noticeable influence is found.

The origin of these observations can be explained by taking into account the phase behavior of the vibrational modes. At the center frequency of the vibrational mode the phase experiences a change of π due to the FT. For both modes, this phase change happens at the respective vibrational center frequency. Therefore both modes are in phase in the frequency range below 555.6 cm^{-1} and also above 606.1 cm^{-1}, but between 555.6 and 606.1 cm^{-1} they experience a phase difference of π and therefore interfere destructively in the frequency domain. This example shows that the phase has to be considered explicitly for the evaluation of vibrational FT spectra in order to obtain correct mode parameters. The phase jump at the center frequency leads to asymmetric line shapes, especially for weak modes in the vicinity of a stronger one. This falsifies the amplitude of the mode and makes an evaluation of the decay time from the width of the Lorentzian impossible.

A long time measurement for the study of wave packet motion requires an experimental setup that has an absolute accuracy of a few femtoseconds over a wide delay time range. This is experimentally demanding, especially for high-frequency vibrational modes. Therefore, considering a more realistic experimental situation also the additional influence of a limited range of delay times has to be taken into account. We plot in Figure 5b the FT spectra $|F(f)|$, $|F(g)|$, $|F(f + g)|$, and $|F(f)| + |F(g)|$ for a delay time range of 0−2000 and 5-fs step size. Because of the finite delay time range, we observe a pronounced $\text{sinc}(\nu)$ behavior for all spectra (with $\text{sinc}(\nu) = \sin(\nu)/\nu$). The distortions in the FT spectrum of the combined modes $|F(f + g)|$ are obvious. Here the parameters of the weak mode at 606.1 cm^{-1} are even more distorted: the vibrational mode is shifted to a vibrational frequency of 611.1 cm^{-1} and also a strong decrease in amplitude is observed.

In a typical pump−probe experiment vibrational wave packet motion is analyzed from FT data sets similar to data set $|F(f + g)|$ in Figure 5b. The influence of the phase shifts and the resulting interference effects have to be explicitly considered for a correct interpretation of the measurements. The example in Figure 5 illustrates the need for an evaluation method that accounts for the phase shift and the $\text{sinc}(\nu)$ structure in the FT spectrum. Such a method is applied in the following for the transient absorption measurement on oxazine 1 presented above (Figure 2).

The algorithm consists of two steps: (i) approximate the complete FT spectrum by a sum of sinc functions with complex amplitudes that represents the individual modes and their phase; (ii) fit the spectral position, amplitude, width, and phase of each mode, using the approximation of the first step i to account for all other neighbored modes. The calculation of the approximated FT spectrum i is explained below.

The limited time range is related in the frequency domain with a convolution of the ideal spectrum $I_{\text{ideal}}(\nu)$ by a sinc function. As a consequence, it is advantageous to expand the FT spectrum $I_{\text{measured}}(\nu)$ of the limited data set (delay time range from 0 to T_0) into a series of sinc functions

$$I_{\text{measured}}(\nu) = \sum_j A_j u_j(\nu) = \sum_j A_j \,\text{sinc}((\nu T_0 - j)\pi) \quad (2)$$

It has been shown that the sinc functions u_j form a complete orthogonal system.[14] For a FT spectrum consisting of a number N of individual bands (of Lorentzian shapes), one can strongly reduce the number of free parameters by the following assumption: The convolution of the ideal FT spectrum with the sinc function is written as a sum of the contributions from the individual bands (shape B_n) with center frequencies ν_n, spectral width w_n, and amplitudes b_n. Each band is than expanded into $(2k + 1)$ sinc function with a limited number of components

$$I_{\text{measured}}(\nu) = I_{\text{ideal}}(\nu) \times \text{sinc}(\upsilon T_0 \pi) = \sum_{n=1}^{N} B_n(\nu_n, w_n, b_n) \times$$

$$\text{sinc}(\upsilon T_0 \pi) \approx \sum_{n=1}^{N} \sum_{m=-k}^{k+1} A_{n,m} \,\text{sinc}(((\nu - \nu_n)T_0 + m)\pi) \quad (3)$$

The measured data set from the transient absorption experiment to which the FT is applied has a finite duration T_0 of 2 ps. Thus finding the coefficients b_n, ν_n, and w_n is a well-posed problem.[14] As the Lorentzians of two well-separated modes are also nearly orthogonal, finding the expansions of several modes ν_n into the respective sinc functions $\text{sinc}(((\nu - \nu_n)T_0 + m)\pi)$ should be a well-posed problem too. As the signal-to-noise ratio is best in the surrounding of the line, one can try to extract as much information on the profile as possible from that region.

From these considerations the following concept for the analysis of well-separated modes is derived: identify the individual modes ν_n and then find the corresponding expansion into sinc functions in the immediate surrounding of the line. Therefore in our analysis we used only three coefficients for each line ($m = -1, 0, 1$).

In the case of a spectrum composed of a number of purely Lorentzian modes as ideal line shape I_{ideal} (ν) from eq 3, thus the following approximation is used

$$\sum_{n=1}^{N} \frac{b_n}{1 - i\,\dfrac{\upsilon - \upsilon_n}{w_n}} \times \text{sinc}(\upsilon T_0 \pi) \cong$$

$$\sum_{n=1}^{N} (A_{n,-1} \,\text{sinc}(((\nu - \nu_n)T_0 - 1)\pi) +$$

$$A_{n,0} \,\text{sinc}(((\nu - \nu_n)T_0)\pi) + A_{n,+1} \,\text{sinc}(((\nu - \nu_n)T_0 + 1)\pi)) \quad (4)$$

To account for the correct phase behavior of approximation the amplitudes $A_{n,-1}$, $A_{n,0}$, and $A_{n,+1}$ are complex numbers. As the sampling points of all three terms in eq 4 are identical, the three complex amplitudes are the values of the nth line profile at these sampling points. For that reason finding the coefficients is a well-posed problem. The fit is only performed in the direct neighborhood of the modes. The advantage of this approximation is the possibility to evaluate not only Lorentzian modes but also more general ones. However, the approximation far away from a mode may be weak. In general that would be the case for strongly damped modes.

For weakly separated lines the sampling points associated with $A_{n,+1}$ and $A_{n+1,-1}$ are in close vicinity. Thus the spectrum at these sampling points is strongly dependent on both $A_{n,+1}$ and $A_{n+1,-1}$. As a consequence, the singular value spectrum of the problem was analyzed and, if required, regularized by truncation. This reduces the information that may be extracted and therefore we concentrate on amplitude, phase, and width of the line. The damping time of the line may be reduced from the latter.

A single mode may be evaluated better by adding a single term of the sum on the right-hand side to the residuum of the approximation. In the case of a purely Lorentzian mode an improvement may be gained by approximating the neighborhood of the mode by a Lorentzian convoluted with a sinc function. The damping times given later are found in this way. It is clear that the results could be refined by iteration. The single steps for the final data analysis are as follows:

(1) The approximate positions of the vibrational modes υ_n are determined using the standard FT spectrum that was averaged over all probe wavelengths in order to improve the signal-to-noise ratio. These positions are used as initial parameters for the fitting routine that models the vibrational spectrum for each probe wavelength separately.

(2) Each vibrational mode is described by the sum of three sinc functions (eq 4, right side). The maxima of the sinc functions with the complex amplitudes $A_{n,-1}$ and $A_{n,+1}$ are shifted by $\pm(cT_0)^{-1}$ relative to the central sinc function with the complex amplitude $A_{n,0}$. To account for asymmetric line shapes, the complex amplitudes $A_{n,-1}$, $A_{n,0}$, and $A_{n,+1}$ are determined as free parameters. Also the vibrational frequencies υ_n are optimized by the fit.

(3) In the final step the line shape of each vibrational mode for each probe wavelength is determined separately by using corrected FT data sets. A Lorentzian convoluted with a sinc-function serves as model function for the fitting procedure (eq 4, left side). Such a corrected FT data set for a distinct vibrational mode υ_k is produced by subtracting the fitted line shapes of all other vibrational modes υ_n with $(n \neq k)$ determined in step ii from the original FT data. By this procedure any oscillatory side maxima or tails due to the spectral shape of neighbored lines have been removed from the FT data set.

This is shown in Figure 6 for the original data set. The FT amplitude (logarithmic scale) of the transient absorption signal is plotted between 510 and 710 cm^{-1} in Figure 6a. The result of the fitting routine using eq 4 is shown in Figure 6b and the remaining residuum in Figure 6c. The corrected data set for the vibrational mode at 606.6 cm^{-1} is presented in Figure 6d. The subtraction method described above leads to the observed shift of the central frequency from 611.1 to 606.6 cm^{-1} and the changed symmetric line shape. Therefore the fitting procedure can now yield the parameters of vibrational modes without influence of neighbored modes.

By this algorithm, the line shape parameters of the vibrational modes in oxazine 1 have been determined (see Figures 4 and 7). In particular the mode at 609 cm^{-1}, that is by a factor of 10 weaker then the nearby lying mode at 560 cm^{-1}, could be evaluated without systematic error by this procedure.

The results of the evaluation for the three strongest lines are shown in Figure 7 as functions of the probe wavelength. The amplitude of the oscillations (Figure 7a) is maximal at about 635 and 670 nm for all modes. A phase shift of π is observed (Figure 7b) at the spectral position of the minimum amplitude

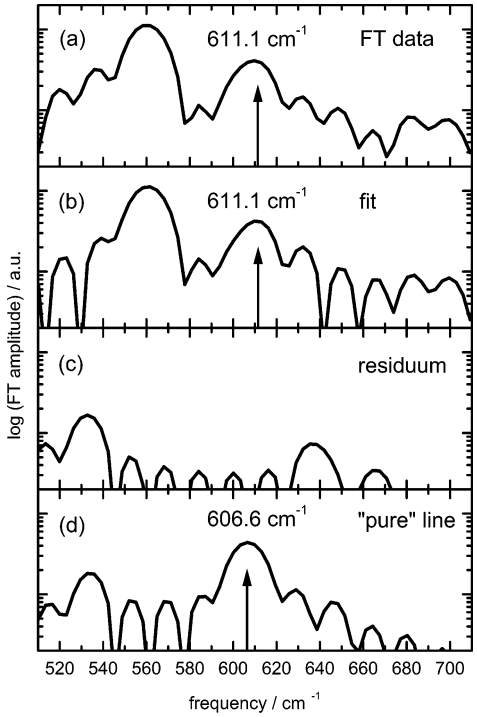

Figure 6. (a) FT amplitude (logarithmic scale) of the transient absorption signal. (b) Fit of data using eq 4. (c) Remaining residuum of the fit. (d) Corrected data set for the vibrational mode at 606.6, according to the evaluation procedure described in the text.

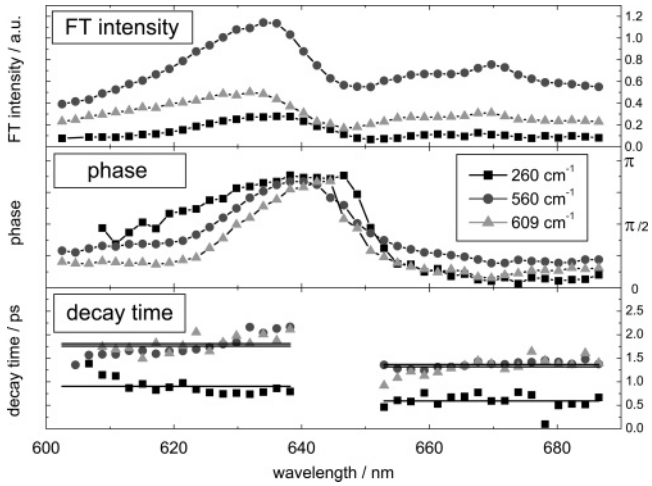

Figure 7. Mode parameters for the three strongest modes 260, 560, and 609 cm^{-1} as a function of the probe wavelength: (a) FT intensity, (b) phase, and (c) decay time of the vibrations are shown. At about 650 nm for all modes a minimum of FT intensity, a phase jump of π, and a change of the decay time is observed.

at about 650 nm (maximum of the cw absorption spectrum). The frequencies of the vibrational modes show no noticeable shift as a function of probe wavelength (not shown here). However, the vibrational decay times (Figure 7c) for all modes in the blue wing between 600 and 640 nm are shortened in the red part of the spectrum (260 cm^{-1}, 0.9−0.6 ps; 560 cm^{-1}, 1.75−1.35 ps; 609 cm^{-1}, 1.8−1.3 ps). In the blue part of the investigated spectral range ground-state wave packets are expected to be dominant, and in the red part excited-state wave packets should play a major role. Therefore the observed difference in decay time is a strong hint for the superposition of ground-state and excited-state wave packet dynamics. To gain further information about the ground-state and excited-state

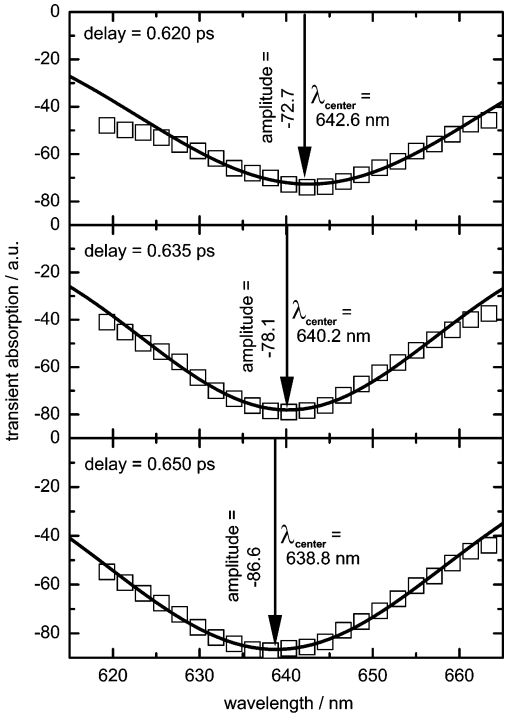

Figure 8. Parametrization of the transient absorption spectra at different delay times. The transient absorption data (shown as squares) are fitted by a Gaussian profile (line) in the spectral range between 625 and 660 nm. For the delay time 0.620, 0.635, and 0.650 ps the Gaussian amplitude and center wavelength are indicated by the arrows.

wave packets, we had a closer look at the time-dependent transient absorption data.

B. Evaluation by a Gaussian Fit of Transient Absorption Spectra in the Time Domain. In Figure 1b it is shown that the transient absorption spectrum can be nicely reproduced by the superposition of steady-state absorption and emission spectra. In the spectral range between 625 and 660 nm close to its peak the transient absorption spectrum is reproduced in a good approximation by a Gaussian representing the spectral signature of the dominant ground-state bleach. This guided us to the following approach. We fit the transient absorption difference spectra for each delay time setting a Gaussian line shape (see Figure 8) and analyze the time dependence of the Gaussian. By this way we gain information averaged over the dominant peak of the transient absorbance change. It should be noted that it is not intended to model ground- and excited-state wave packet motion by this approach. Instead, the experimentally observed main features of the complex two-dimensional data set (Figure 2) can be described in a clear representation by this procedure.

The obtained fit parameters are peak amplitude, peak position, and width of the Gaussian as a function of delay time, as shown in Figure 9. At first sight the typical oscillatory behavior with a beating period of about 650 fs is found for all three parameters. The result of the FT analysis of the time dependence is also shown in Figure 9 as insets. Obviously the vibrational modes of the molecule are found for the three parameters as a result of the evaluation method described above (see Figure 4). However, by analysis of amplitude, spectral position, and spectral width separately, further information is available.

The main effect of wave packet motion on an optical transition is often described in a simple first-order approximation as a modulation of its spectral position. Indeed we find a change in peak position, which oscillates between 637 and 643 nm (Figure 9b). Also the spectral width is found to change between

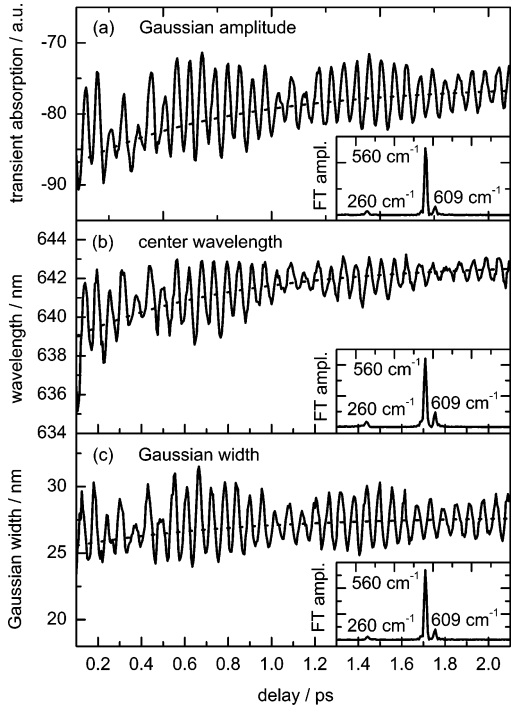

Figure 9. Result of the Gaussian fit as in Figure 7 for the delay times between 0.1 and 2.1 ps. (a) amplitude of the Gaussian, (b) center wavelength of the Gaussian, and (c) width of the Gaussian profile as a function of delay time. The three parameters oscillate with the same frequency spectrum as shown in the insets. The dotted lines (as guides to the eye) represent the evolution of the averaged behavior of the three mode parameters, as described in the text.

25 and 31 nm (Figure 9c). This leads to the experimental observation that the FT intensity in Figure 7 reaches its maximum (about 635 nm), where the spectral slope of the transient absorption spectrum is steepest (Figure 1b). However, this would also suggest that at the spectral position of the optical transition maximum (643 nm, Figure 1b) the FT intensity of this mode should be exactly zero. This however is not observed for the FT intensity in Figure 7.

The reason for that behavior is the decrease and increase of the transition intensity with a modulation amplitude of about 10% (see Figure 9a). This effects the oscillation on the transient absorption signal strongest at the spectral maximum position of the optical transition (643 nm). Therefore the modulation of the transition dipole moment due to the wave packet motion can lead to similarly strong oscillations in the optical probe signal as the modulation of its spectral position. This effect can complicate for example the determination procedure for the correct phase of the oscillations.

4. Discussion

In the following the results for the wave packet dynamics initiated by a transform limited ultrashort light pulse are discussed. The wavelength-dependent evaluation of the wave packet motion for the three modes 260, 560, and 609 cm^{-1} is seen in Figure 7. We assume that the absorption and emission spectra are changed due to the motion along the respective vibrational coordinate. This leads to a wavelength-dependent modulation of the transient absorption signal with the respective vibrational frequency that is proportional to the derivative of the transient absorption spectrum. That behavior explains well that the maxima of the Fourier transformed data of the three modes are at 635 and 670 nm, where the slope of the transient absorption spectrum is at its maximum (see Figure 7a). Also it explains the observed phase shift of the oscillations at the transient absorption maximum (see Figure 7b). The shift in the spectral position of the transient absorption signal is also confirmed by the evaluation method in time domain using Gaussian fits presented in Figure 9b.

Nevertheless it is assumed that at the central wavelength, where the transient absorption spectrum peaks, the signal modulation due to the wave packet reaches not only its minimum but vanishes. This can obviously not be observed for the presented data. Therefore a further signal has to contribute to the modulation of the transient absorption due to wave packet motion. This signal is also identified from the Gaussian fit data evaluation in the time domain as a periodic change of the transition dipole moment (Figure 9a), which contributes to the oscillation most at the spectral maximum position. Therefore the spectrum of the FT amplitude (Figure 7a) can be modeled as a superposition of the transient absorption spectrum and its first derivative. This should be kept in mind as a possible mechanism that may lead to a complex behavior of the phase as a function of the probe wavelength. Therefore an assignment of vibrational modes to the ground or excited state only relying on the phase information seems to be not sufficiently accurate in the overlap region of the transient absorption and emission spectrum. Further studies on the assignment were carried out with the help of chirped excitation pulses.[15]

Also a closer look at the Gaussian fit data (Figure 9) reveals some interesting details about the behavior of ground-state wave packets in oxazine 1. Bleach intensity, spectral width, and spectral position are modulated in phase: the strongest bleach is observed in the blue part of the spectral range, where the spectral width of the Gaussian is narrow. A similar behavior can be observed when the averaged evolution of the Gaussian parameters is analyzed (dotted lines as guide to the eye in Figure 9). The average bleach intensity (Figure 9a) decreases over the shown time range of 2 ps. This is associated with a slight increase of the spectral width (Figure 9c) and a red shift of the spectral position from about 639 to 643 nm. This means that the maximum transition probability is found in the blue wing of the bleach spectrum, where also a high Franck−Condon factor is expected. When the modulation of the transient absorption signal due to the decay of the wave packet motion decreases, the spectral position of the Gaussian evolves to the steady-state absorption maximum of 643 nm. The decay of the wave packet is also monitored by the decay of the modulation of the spectral width of the Gaussian. Additionally a slight increase of the spectral width of the Gaussian is observed for later delay times (dotted line in Figure 9) to the value observed for the long-lived nanosecond kinetic (see Figure 1b). It should be noted that also larger values for the spectral width were observed in the oscillatory signal, because due to the wave packet motion more vibrational excited states contribute to the wave packet.

The different vibrational decay times (Figure 7c) observed in the blue (600−640 nm) and red part (650−690 nm) of the spectrum for the modes 260, 560, and 609 cm^{-1} are a strong indication that the wave packets observed in these two spectral regions are propagating on different parts of the potential-energy surfaces. Therefore they will experience different decay mechanisms. The faster decay times observed for the vibrational wave packets in the excited state can be explained by a weak solvent−solute interaction. The system oxazine/methanol is photoexcited when it is in a collective equilibrium geometry in the electronic ground state. After generation of the ground-state wave packet this equilibrium geometry is not changed. However, for the case

of a wave packet in the excited state solvent molecules will start to realign to a new equilibrium geometry. Therefore decoherence is induced in the molecular system and this additional dephasing mechanism leads to a shorter lifetime of the excited-state wave packet.

Also experimental and theoretical work was presented in the literature,[16] where different decay times of vibrational wave packets were explained in a way that higher-lying vibrational states show a faster relaxation. Therefore it was concluded that wave packets near the bottom of the ground- or excited-state potential-energy surface exhibit slower decay times and wavelength-dependent decay times are expected. According to our experimental data, we observe only one decay time for each vibrational mode in the blue part (600−640 nm) and another decay time in the red part (650−690 nm) of the investigated spectral range. Therefore, in the case of oxazine 1 an explanation of the different decay times due to ground- and excited-state wave packets is stronger supported by our experiments.

By comparison with the steady-state spectra (Figure 1) it can be concluded that between 600 and 640 nm a ground-state wave packet is observed and in the range 650−690 nm the excited-state wave packet participates on the oscillations. The evaluation of these decay times even for the weak modes at 260 and 609 cm^{-1} was performed with the improved evaluation algorithm in frequency domain as presented above. Therefore any systematic errors as demonstrated for simulated data sets in Figure 5 could be avoided. A confirmation for this assignment was obtained independently from experiments with chirped pulse excitation.[15]

5. Conclusion

We presented spectrally resolved transient absorption measurements of oxazine 1 in methanol with 15 fs pulses. Oscillatory signal components due to wave packet motion was observed with vibrational frequencies up to about 1300 cm^{-1}. The data were analyzed directly by fitting the transient absorption spectra for each delay time by Gaussian line shapes. The signal components of the oscillatory signal due to the resonance frequency shift and the change in the transition dipole moment was determined. We also presented an advanced evaluation algorithm of the FT data set taking into account the decay time and sinc structure of the FT data. In an iterative approach this algorithm allows to determine the parameters of neighbored modes without systematic error. This evaluation scheme is promising for the correct evaluation of vibrational FT spectra with several neighbored modes.

Acknowledgment. We thank A. Peine, P. Gilch, and W. Zinth for fruitful discussion. This project was funded by the Deutsche Forschungsgemeinschaft (SFB 533).

References and Notes

(1) Garraway, B. M.; Suominen, K. A. *Rep. Prog. Phys.* **1995**, *58*, 365.
(2) Zewail, A. H. *J. Phys. Chem.* **1996**, *100*, 12701.
(3) Domcke, W.; Stock, G. Theory of ultrafast nonadiabatic excited-state processes and their spectroscopic detection in real time. In *Advances in Chemical Physics*; Prigogine, I., Rice, S. A., Eds.; John Wiley & Sons: 1997; Vol. 100.
(4) Brixner, T.; Gerber, G. *Chem. Phys. Chem.* **2003**, *4*, 418.
(5) Pollard, W. T.; Lee, S. Y.; Mathies, R. A. *J. Chem. Phys.* **1990**, *92*, 4012.
(6) Hasche, T.; Ashworth, S. H.; Riedle, E.; Woerner, M.; Elsaesser, T. *Chem. Phys. Lett.* **1995**, *244*, 164.
(7) Baum, P.; Lochbrunner, S.; Riedle, E. *Appl. Phys. B* **2004**, *79*, 1027−1032.
(8) Wilhelm, T.; Piel, J.; Riedle, E. *Opt. Lett.* **1997**, *22*, 1494.
(9) Riedle, E.; Beutter, M.; Lochbrunner, S.; Piel, J.; Schenkl, S.; Sporlein, S.; Zinth, W. *Appl. Phys. B* **2000**, *71*, 457.
(10) Carson, E. A.; Diffey, W. M.; Shelly, K. R.; Lampa-Pastirk, S.; Dillman, K. L.; Schleicher, J. M.; Beck, W. F. *J. Phys. Chem. A* **2004**, *108*, 1489.
(11) Lanzani, G.; Zavelani-Rossi, M.; Cerullo, G.; Comoretto, D.; Dellepiane, G. *Phys. Rev. B* **2004**, *69*.
(12) Baigar, E.; Braun, M.; Peine, A.; Konjaev, V.; Zinth, W. *Convenient tunability of sub-10 fs-pulses in the visible range*; Ultrafast Phenomena: Vancouver, 2002.
(13) Engleitner, S.; Seel, M.; Zinth, W. *J. Phys. Chem. A* **1999**, *103*, 3013.
(14) Gamo, H. Matrix treatment of partial coherence. In *Progress in Optics*; Wolf, E., Ed.; North-Holland Publishing Co.: 1964; Vol. III.
(15) Malkmus, S.; Dürr, R.; Sobotta, C.; Pulvermacher, H.; Zinth, W.; Braun, M. *J. Phys. Chem. A* **2005**, *109*, 10488.
(16) Bardeen, C. J.; Wang, Q.; Shank, C. V. *J. Phys. Chem. A* **1998**, *102*, 2759.